

EIC R&D PROGRESS REPORT

REPORTING PERIOD: **JANUARY 2014** TO **JUNE 2014**

RD2013-2:
A Compact Magnetic Field Cloaking Device

K. Boyle[†], K. Capobianco-Hogan[‡], R. Cervantes[‡], J. Chang[‡], B. Coe[‡],
K. Dehmelt[‡], A. Deshpande^{‡*}, N. Feege^{‡*}, Y. Goto[§], R. Gupta[¶],
T. K. Hemmick[‡], P. Karpov[‡], Y. Ko[‡], T. LaByer[‡], R. Lefferts[‡], A. Lipski[‡],
E. Michael[‡], I. Nakagawa[§], J. Nam[‡], B. Parker[¶], V. Ptitsyn[¶], A. Quadri[‡],
J. Seele[†], K. Sharma[‡], I. Yoon^{||}

June 27, 2014

*Co-Principal Investigators

E-mail: Abhay.Deshpande@stonybrook.edu, Nils.Feege@stonybrook.edu

[†]RIKEN BNL Research Center

[‡]Stony Brook University, SUNY

[§]RIKEN

[¶]Brookhaven National Laboratory

^{||}Seoul National University

1 Objectives

We planned to continue the realization and test of a magnetic field cloaking device with dimensions close to those we expect for an experiment like an EIC detector. This includes extending our test set-ups and testing and procuring suitable materials for the prototype construction from commercial suppliers.

2 Timeline

Figure 1 shows the timeline for this project as it was laid out in the previous report. The green bars indicate our progress on the different parts.

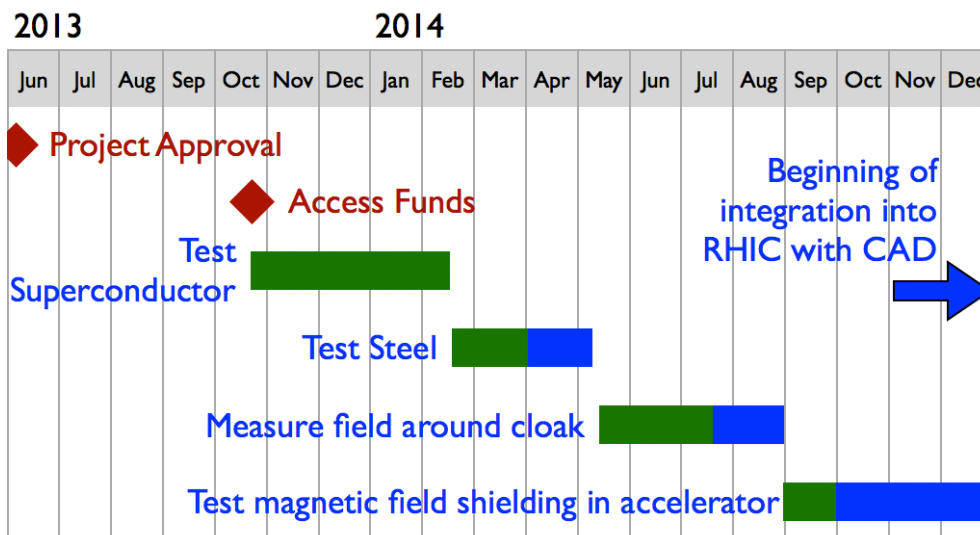


Figure 1: Project timeline.

This report presents our results from testing the superconductor tape which we use for our current magnetic cloak prototypes.

The addition of the steel layer takes longer than expected because we found that cold-working 302 stainless steel to tune the permeability of this material to use it for the cloak is not a viable option for us. Therefore, we are exploring a different approach: creating a sheet from a compound of 430 stainless steel powder and aluminum powder and tuning the permeability of this sheet by adjusting the fraction of steel powder in the mixture.

We measured the effect of a superconducting shielding layer on the surrounding magnetic field. So far, we only did these measurements in a small Helmholtz coil setup at lower fields compared to those initially planned. The

reason for this are limitations in the commissioning of the CDS solenoid magnet.

In parallel with these ongoing activities, we built a 1.3 m prototype of a superconducting shielding cylinder to demonstrate its capability to shield a charged particle beam from a magnetic field. The beam line at Stony Brook and our beam position monitoring setup are ready as well. We will start these tests as soon as we complete the system to cool the superconductor inside the beam pipe.

We followed up on the idea to evolve our superconductor cylinders into a magnetic field shield for the transfer line from the polarized He3 source to EBIS and will further explore this option over the next weeks.

3 Achievements

With 10 Stony Brook undergraduate students (K. Capobianco-Hogan, J. Chang, B. Coe, P. Karpov, T. LaByer, Y. Ko, E. Michael, J. Nam, A. Quadri, K. Sharma), one MSI student (R. Cervantes) and a guest student from Seoul National University (I. Yoon) we have made significant progress towards accomplishing our objectives. We successfully

- measured the shielding performance of one to four layers of our superconductor tape up to 500 mT and confirmed (partial) shielding over the full range (Sec. 3.1),
- evaluated different wrapping options for the superconductor tape to form a cylinder (Sec. 3.2),
- established a method to measure the magnetic permeability of a metal cylinder and laid out a new procedure to create ferromagnetic sheets of the permeability we need (Sec. 3.3),
- mapped the field inside and around a superconducting cylinder to quantify the effect of the superconductor on the field (Sec. 3.4),
- constructed a 1.3 m long superconductor cylinder and prepared the Van de Graaff accelerator beam line at Stony Brook to test the magnetic field shielding performance of this cylinder with a proton beam (Sec. 3.5).

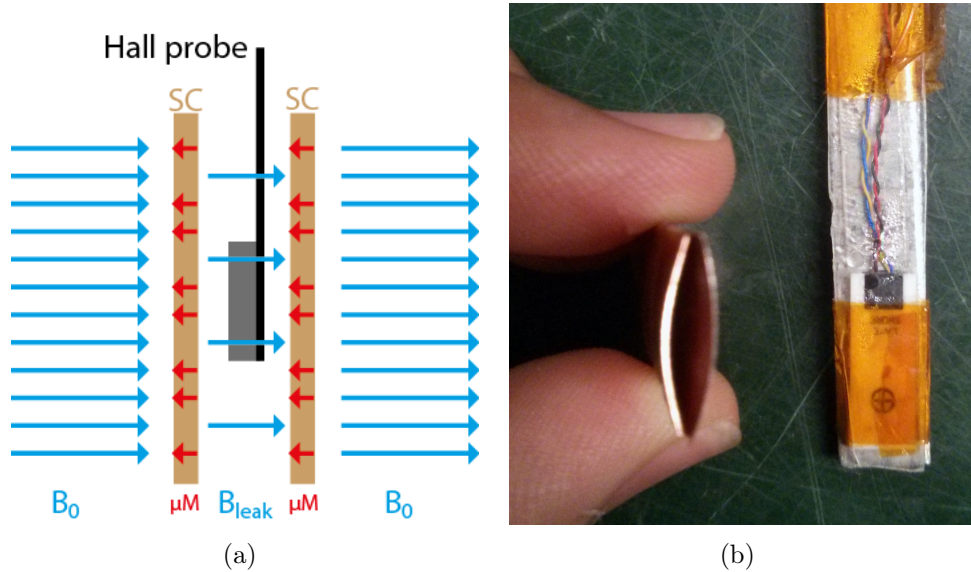


Figure 2: (a) The setup for testing our superconductor tape. We apply an external field B_0 measure the field B_{leak} between two layers of superconductor SC . (b) Photo of a superconductor sheath next to our Hall probe.

3.1 Superconductor Tape Properties

We procured 35 m of 12 mm wide type II superconductor tape (SuperPower M3-1003-1, 65 μm Cu stabilizer) with a critical current above 420 A. We measured the field shielding properties of the tape itself while minimizing fringe fields by forming a superconductor sheath from two 4.5 cm long strips of the tape and inserting our Hall probe into it. We then submerged the probe and the superconductor in a liquid Nitrogen bath inside a dipole magnet and measured the field between the superconductor layers, B_{leak} , for one minute at external magnetic fields B_0 from 1 mT to 500 mT. Figure 2(a) and 2(b) illustrate the setup.

The currents induced in the superconductor create an effective magnetization μM of the superconductor which shields the field. At fields above the first critical field B_{c1} , parts of the superconductor become normally conductive and some of field reaches the Hall probe. Because magnetic fields can diffuse through the grains of a high temperature superconductor, B_{leak} can be greater than zero even when B_0 is below B_{c1} . This effect is known and also introduces a logarithmic time dependence of B_{leak} [1].

Figures 3(a) and 3(b) show measurements of B_{leak} at $B_0 = 5$ mT and $B_0 = 21$ mT. The 21 mT measurement clearly shows a time dependence of B_{leak} , which is not visible at 5 mT. If there is a time dependence, we fit a

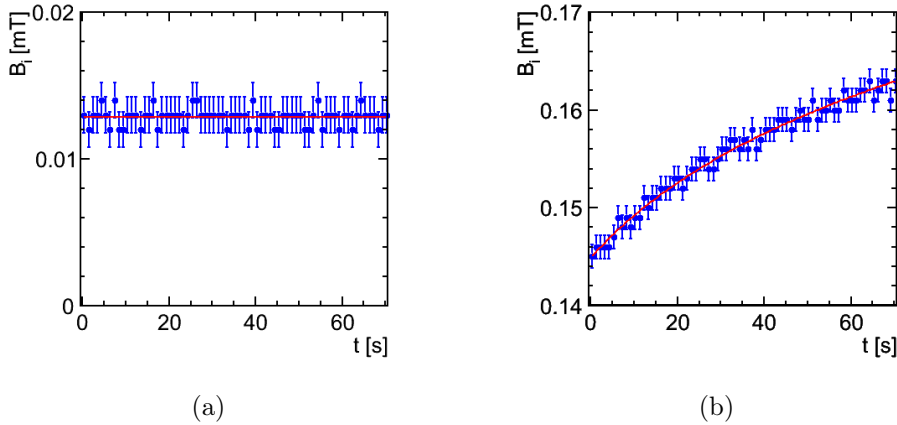


Figure 3: (a) Measured shielded field B_{leak} as a function of time t at (a) 5 mT and (b) 21 mT external field B_0 .

logarithmic function to the data and use the extrapolation of the function to one year as value for B_{leak} . Otherwise, we use the mean. Increasing the measurement time from one minute to an hour yields comparable fit and extrapolation results.

The shielded field B_{shield} is the difference between B_0 and B_{leak} and equals the superconductor magnetization μM . Figure 4(a) shows B_{shield} as a function of B_0 between 1 mT and 500 mT. The data follow a curve typical for type II superconductors: At low fields, B_{shield} is equal to B_0 . After B_0 rises above the critical field B_{c1} , the shielded field decreases. We attribute the deviation from 100% shielding below this point to fringe fields and the field diffusion through the superconductor itself. At 500 mT, we still measure a shielding of 6 mT, which means that this field is still below the second critical field. This indicates that we can increase the maximum shielded field at least up to 500 mT by increasing the number of superconductor layers.

We tested up to four layers of the superconductor sheath and Fig. 4(b) shows the maximum fields B_{95} for which we observe 95% shielding as a function of superconductor layers. This confirms the improvement of shielding performance with additional layers. The plot also indicates a linear relation between shielded field and number of layers and that we need 36 layers to reach 95% shielding at 500 mT. We will add more measurements for a more reliable extrapolation.

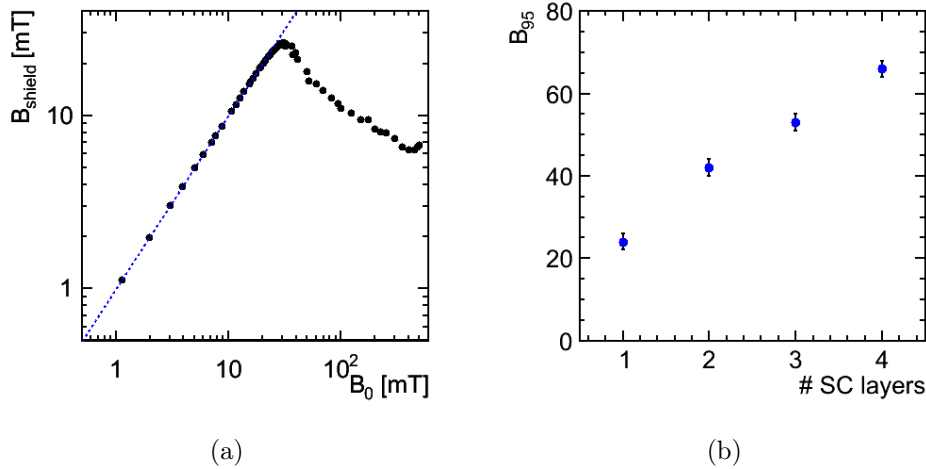


Figure 4: (a) Measured shielded field B_{shield} as a function of external field B_0 . The dashed line illustrates $B_{shield} = B_0$. (b) Maximum field B_{95} for which we measure 95% shielding as a function of superconductor layers.

3.2 Tape Wrapping Options For SC Cylinders

We tried two options for wrapping our superconductor tape around an Aluminum core of 12.85 mm outer diameter to create a superconducting cylinder: Wrapping a single strip of the tape in a helix around the core ('helix' option) and using multiple strips placed vertically along the cylinder with an overlap of about 2 mm ('vertical' option). Figures 5(a) and 5(b) illustrate these options. Both styles cover a length of 7.4 cm on the Aluminum core and are held in place by Kapton.

Figure 6(a) illustrates our test setup for evaluating the two cylinders. We placed the superconducting cylinders in a liquid Nitrogen bath inside a pair of Helmholtz coils (5451 Electromagnet GMW Magnet Systems, 05). A rig made from 80/20 material supports both the cylinders and a cryogenic Hall probe mounted on an Aluminum bar. The probe can move inside the superconducting cylinder along its center axis.

Fig. 6(b) shows the fields measured inside the superconducting cylinder at room temperature (no shielding) and at liquid Nitrogen temperature for one and two layers of both wrapping styles. We chose a field of only 2 mT for this test because it is considerably lower than the critical field for the superconductor tape and we can assume no field passes through the superconductor itself. Therefore, we measure only fringe fields entering the cylinder from the sides or through gaps in the superconductor tape wrapping.

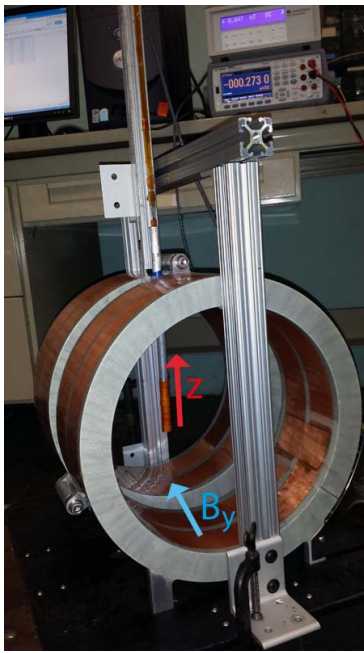
The measurements for one layer of the helix wrapping show a distinct



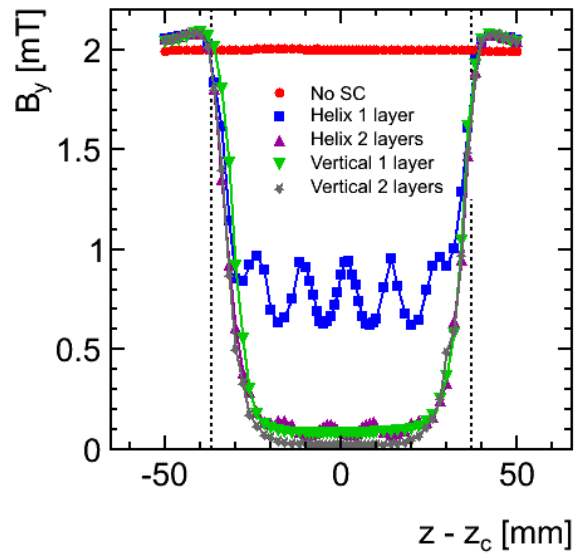
Figure 5: (a) 'Helix' and (b) 'vertical' superconductor wrapping option.

structure of maxima and minima. The six minima correspond to the six turns of superconductor tape for the helix wrapping and the 5 maxima correspond to the gaps between adjacent turns. When wrapping multiple helix layers we make sure that the top layer covers the gaps of the previous layer. Therefore, the effect of these gaps is less pronounced for two layers of helix wrapping. The vertical strip wrapping for one and two layers shows much less fringe field leaking through the superconductor layers and no position dependent structure of the field inside the cylinder. Therefore, this wrapping style appears to be the better option for shielding and we use it for our other prototypes.

We tested the shielding of both wrapping options with two layers in our dipole with a setup analog to the one described in Section 3.1. Figure 7 compares the shielded field B_{shield} (measured at the center of the superconducting cylinders) to the B_{shield} for a sheath made from a single tape layer as a function of external field B_0 . The plot shows that the 'vertical' options shields external fields better than the 'helical' options. However, the shielding from both cylinders appears to be considerably lower than the shielding we measured for the tape itself. This feature may be the result of fringe fields leaking into the cylinders from the sides. Another possible reason is



(a)



(b)

Figure 6: a) Setup to measure the field inside the superconducting cylinder at various positions z along the cylinder axis. (b) Field measured along the axis of superconducting cylinders made from one and two layers of 'helix' and 'vertical' type wrapping.

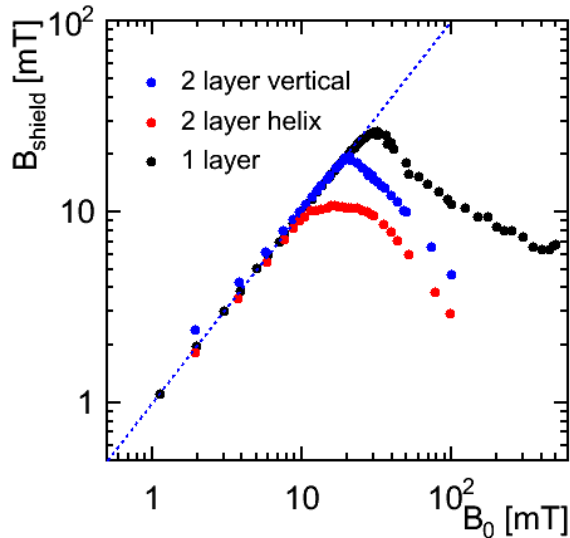


Figure 7: Measured shielded field B_{shield} as a function of external field B_0 for a sheath made from a small tape sample and two layers of 'helix' and 'vertical' style wrapped superconducting cylinders. The dashed line illustrates $B_{shield} = B_0$.

that wrapping the tape around the Aluminum core effectively damages the superconductor in the tape and therefore reduces its shielding performance. We will do a more systematic study of the effect of wrapping and handling and possible damage on the tape performance.

3.3 Ferromagnetic Layer Properties

In order to measure the relative permeability μ_r of a ferromagnetic test sample, we formed the sample into a cylinder of inner radius a and outer radius b . We applied a homogeneous field \mathbf{B}_{ext} using the Helmholtz coil and measured the internal field \mathbf{B}_{int} . The relation

$$\mathbf{B}_{int}(r < a) = \frac{4\mu_r b^2}{(\mu_r + 1)^2 b^2 - (\mu_r - 1)^2 a^2} \mathbf{B}_{ext} \quad (1)$$

between \mathbf{B}_{int} and \mathbf{B}_{ext} and yields μ_r [2].

Our initial plan was to use cold-worked 302 stainless steel as our ferromagnetic layer. Figure 8 shows the measured permeability of our stainless steel sample after demagnetizing it by heating it above the Curie temperature. A permeability of 1.5 is typical for 302 stainless steel after 30% of

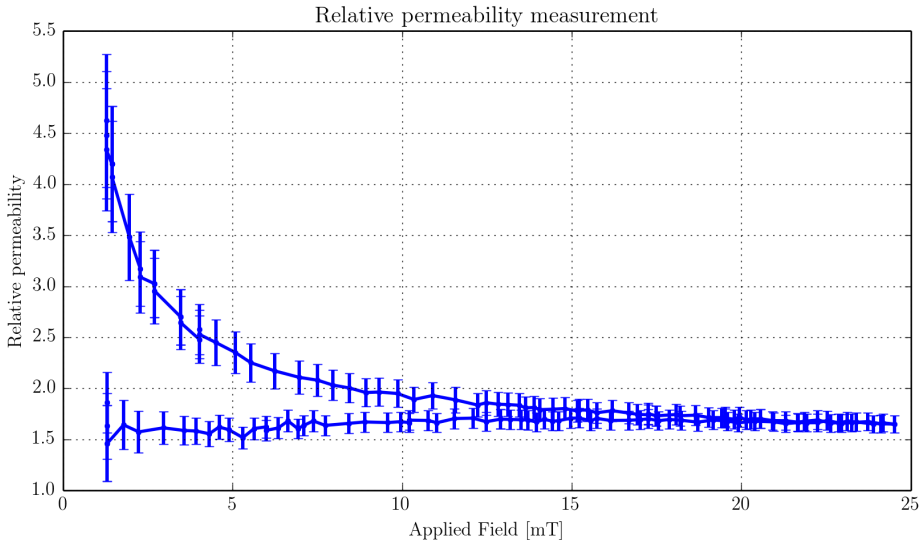


Figure 8: Magnetic permeability of a 302 stainless steel sample. The effects of hysteresis are clearly visible.

cold work reduction, so the used method gives reasonable results. However, stainless steel has a relatively high coercivity, which results in the hysteresis effect visible in the figure and would compromise the cloak performance. In addition, the hardness of our stainless steel sample made it difficult to cold work with our available equipment.

Low permeability, low coercivity ferromagnets are not commercially available, because industry prefers either high permeability, high coercivity ferromagnets for magnetic shielding or low coercivity, low permeability ferromagnets for digital memory. We are currently exploring an option to use a composite material consisting of a ferritic 430 stainless steel (low coercivity and $\mu_r \approx 800$) and Aluminum ($\mu_r = 1$) powder. By adjusting the fractional volume of stainless steel with aluminum, we can tune the effective permeability of the compound.

Figure 9 shows our first test of melting the aluminum powder and rolling it with a roller press to create a flat sheet for a cloak layer. We will do tests with varying fractions of 430 stainless steel powder to measure how it affects the permeability.

As an initial guess, we will use the Maxwell-Garnett Formula

$$\mu_{eff} = \mu_e + 2\mu_e \frac{\mu_i - \mu_e}{\mu_i + \mu_e - f(\mu_i - \mu_e)} \quad (2)$$

for calculating the effective permeability, where μ_{eff} is the effective permeability, μ_i is the permeability of randomly located circular cylinders in a



Figure 9: A sample of our Aluminum made from Aluminum powder before and after using the roller press to form it into a flat sheet.

homogeneous environment with permeability μ_e and occupy a volume fraction f [3].

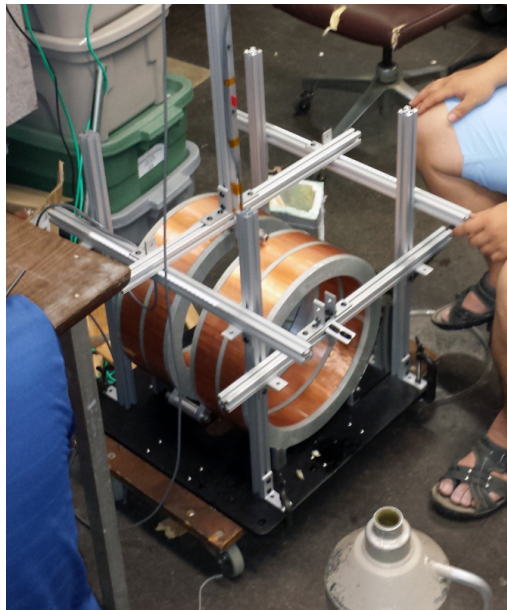
3.4 Superconductor Effect On Magnetic Field

For testing the effects of our superconductor on the surrounding field, we built a superconducting cylinder with 4 layers of 'vertical' tape wrapping around an Aluminum core. This cylinder is 9 cm long and has an outer diameter of 3.5 cm (see Fig. 10(a)).

Figure 10(b) shows another 80/20 rig we constructed around a pair of Helmholtz coils to measure the field inside and around this cylinder. The rig allows us to move a cryogenic Hall probe in all three Cartesian directions (x , y , z) inside and around the cylinder. Figure 11(a) illustrates the expected field lines around the superconductor in the x - y plane and the two lines along which we measured the field. Figure 11(b) shows a measurement of the field along the axis of the cylinder, while Figs. 11(c) and 11(d) show the measurements along x for two different y positions of the probe. All three figures also indicate the Helmholtz coil field we measured when no superconductor was present. As expected, there is no field inside the superconducting cylinder, while the field lines are bent around the cylinder so that we measure a higher field on the sides and a lower field in front of the cylinder (looking in the direction of the magnetic field).



(a)



(b)

Figure 10: (a) Superconductor cylinder with four layers of 'vertical' wrapping. (b) Setup for measuring the magnetic field inside and around a superconducting cylinder in a pair of Helmholtz coils.

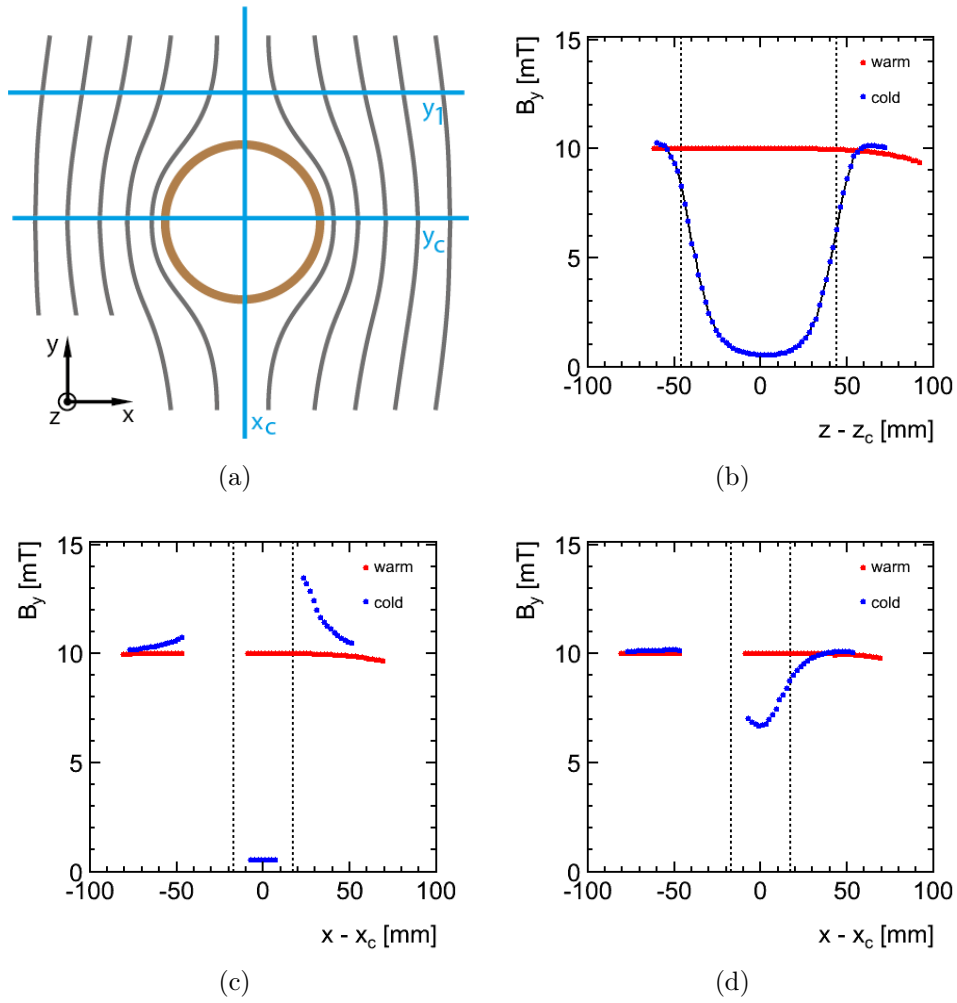


Figure 11: (a) Schematic of magnetic field line bending around a superconducting cylinder. (b) Measurement along the cylinder axis ($x = x_c$, $y = y_c$). (c) Measurement along x crossing the center of the cylinder ($y = y_c$). (d) Measurement along x outside the cylinder ($y = y_1$).

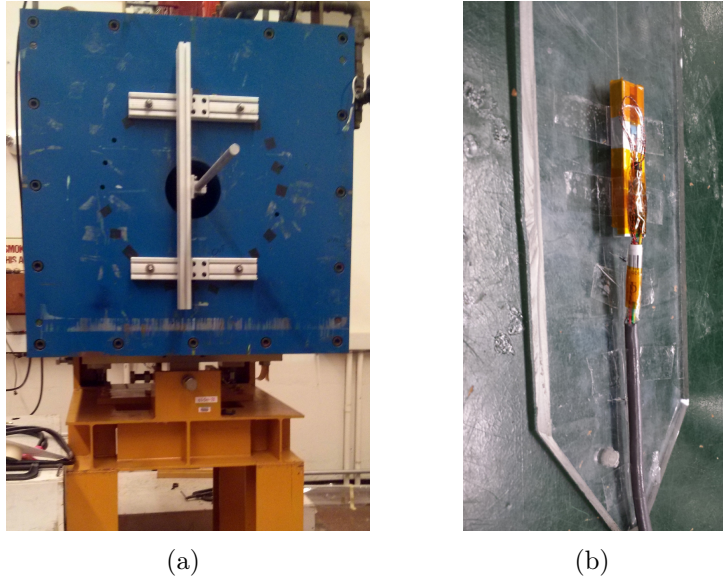


Figure 12: (a) CDS magnet field mapping setup. (b) Rotor with attached Hall probe.

3.4.1 CDS Magnet Field Map

As explained in the last report, we currently cannot commission the CDS magnet at Stony Brook at its full power. However, we used a small power supply that provided a fraction of the full field to test the magnet operation and map the field. Figure 12(a) shows the field mapping setup we constructed. A rotor (Fig. 12(b)) is connected to a bar which runs along the axis of the magnet. A Hall probe is attached to the rotor at varying radii and the bar can be rotated, moved along the magnet axis, and perpendicular to the axis. This allows to measure the field at each point inside the magnet.

Figure 13 shows our measurement of the magnetic field along the center of the CDS magnet at a maximum field strength of 140 mT. We created a COMSOL simulation of the magnet and the prediction of the simulation, which is also shown in this figure, agrees with our measurement within less than 1%. The figure also includes a previous measurement of the field of this magnet (done at the full 500 mT peak field) as reference [4]. This previous measurement indicates a more homogeneous field than our measurements and simulations and we are still investigating possible origins of this difference.

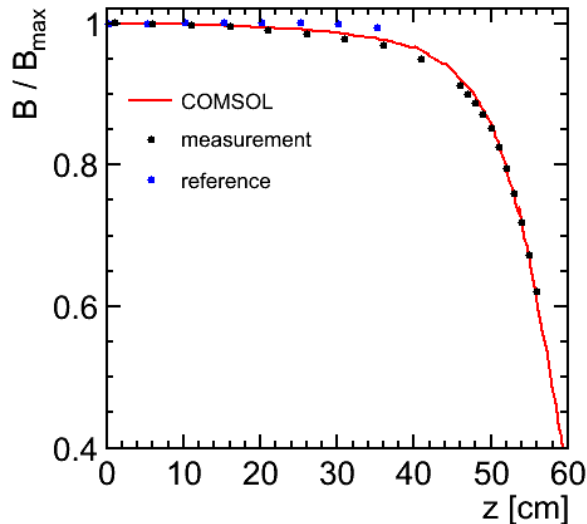


Figure 13: Magnetic field along the center axis of the CDS magnet: Our COMSOL simulation, our measurements done with our field mapping setup, and the reference measurement from [4].

3.5 SC Shield Test In The Van de Graaff Accelerator

Figure 14 shows our measurement of the field along the beam pipe at a low current setting. The maximum field is adjustable up to 500 mT. The field is very homogeneous along the beam line with a sharp rise and fall at the ends of the magnet. Based on this we chose to make our superconductor shield 1.3 m long to cover the whole magnet.

We used the 'vertical' wrapping option to build a 1.3 m long superconductor shielding cylinder with four layers which is pictured in Fig. 15. We are still finalizing our design for a cooling system for the superconductor shield inside the beam pipe.

4 Future

Our next steps are to

- continue our tests as planned, in particular to add the ferromagnetic layer to the cloak prototype, do systematic tests of the impact of handling and wrapping the superconducting tape on the tape performance, and test the 1.3 m prototype in the Van de Graaff beam line,

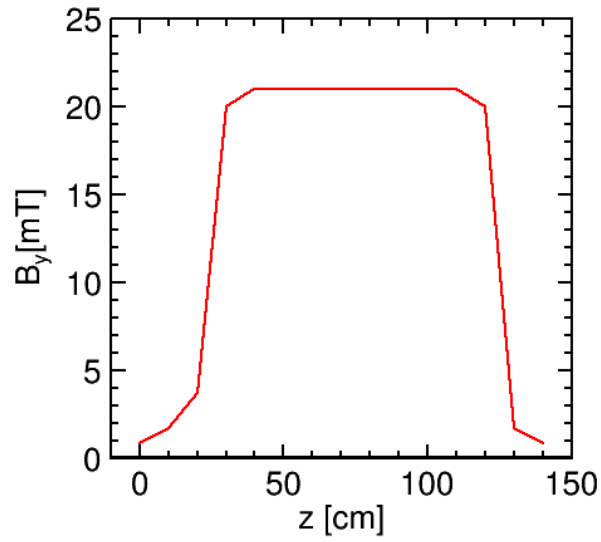


Figure 14: The field of the dipole magnet in the Van de Graaf accelerator beam line.



Figure 15: Superconductor shield for test in the Van de Graaff accelerator at Stony Brook (14 mm inner diameter, 1.3 m long).

Table 1: Current budget request.

Item	Cost [\$]
High-temperature superconductor tape	24,000
Liquid Nitrogen	1,000
Total Direct Cost	25,000
Total Indirect Cost	14,500
Total Request	39,500

- investigate better methods for wrapping long superconducting cylinders from superconductor tape,
- further explore how well our superconductor cylinders would be suitable as a magnetic field shield for the polarized He3 source,
- add ten more layers to the Van de Graaff prototype to improve its shielding performance,
- collaborate with BNL SMD to test our tape at liquid Helium temperature and also test low-temperature superconductor sheets,
- explore possible collaboration with BNL CAD for beam line integration of a magnetic cloak prototype.

5 Additional Budget Request

Table 1 summarizes our current budget request. We are asking for funds to procure enough superconductor tape to add ten layers to our 1.3 m long superconductor shield prototype. Furthermore, we need funds for additional liquid Nitrogen supplies to continue our superconductor tests.

At this time we are not requesting an additional budget for labor. However, for the following funding period we would like to ask for \$ 80,000 for the salary of a graduate student for one year and a post-doc for three months. At that time we may also need about \$ 15,000 to procure low-temperature superconductor sheets (niobium-titanium) and liquid Helium supplies.

References

- [1] A. D. Havenhill et al., *Magnetic Flux Diffusion Through HTS Shields*. IEEE Transactions on Applied Superconductivity, Volume 8, Issue 2, 1998.
- [2] A. Zangwill, *Modern Electrodynamics*. Cambridge University Press, ISBN 0521896975, 2012.
- [3] H. Waki et al., *Estimation of effective permeability of magnetic composite materials*. IEEE Transactions on Magnetics, Volume 41, Issue 5, 2005.
- [4] J. P. Nakano, *Study of Double-Lambda Hypernuclei by Using Cylindrical Detector System*. CNS-REP-28, 2000.